# Valproic acid inhibits the growth of HeLa cervical cancer cells via caspase-dependent apoptosis

BO RAM HAN, BO RA YOU and WOO HYUN PARK

Department of Physiology, Medical School, Research Institute for Endocrine Sciences, Chonbuk National University, Jeonju 561-180, Republic of Korea

Received July 24, 2013; Accepted August 26, 2013

DOI: 10.3892/or.2013.2747

**Abstract.** Valproic acid (VPA) as a histone deacetylase (HDAC) inhibitor has an anticancer effect. In the present study, we evaluated the effects of VPA on the growth and death of HeLa cervical cancer cells in relation to reactive oxygen species (ROS) and glutathione (GSH). Dose- and time-dependent growth inhibition was observed in HeLa cells with an $IC_{50}$ of approximately 10 mM at 24 h. DNA flow cytometric analysis indicated that 10 mM VPA induced a G2/M phase arrest of the cell cycle. This agent also induced apoptosis, which was accompanied by the cleavage of PARP, the activation of caspase-3, -8 and -9, and the loss of mitochondrial membrane potential (MMP; $\Delta\Psi_m$). All the tested caspase inhibitors significantly prevented HeLa apoptotic cell death induced by VPA, whereas TNF-α intensified the apoptotic cell death. With respect to ROS and GSH levels, VPA increased ROS levels and induced GSH depletion. However, N-acetyl cysteine (NAC; an antioxidant) and L-buthionine sulfoximine (BSO; a GSH synthesis inhibitor) did not significantly affect cell death in VPA-treated HeLa cells. In conclusion, VPA inhibits the growth of HeLa cervical cancer cells via caspase-dependent apoptosis and the growth inhibition is independent of ROS and GSH level changes.

*Correspondence to:* Professor Woo Hyun Park, Department of Physiology, Medical School, Research Institute for Endocrine Sciences, Chonbuk National University, Jeonju 561-180, Republic of Korea
E-mail: parkwh71@chonbuk.ac.kr

*Abbreviations:* VPA, valproic acid; HDAC, histone deacetylase; ROS, reactive oxygen species; GSH, glutathione; Z-DEVD-FMK, benzyloxycarbonyl-Asp-Glu-Val-Asp-fluoromethylketone; Z-IETD-FMK, benzyloxycarbonyl-Ile-Glu-Thr-Asp-fluoromethylketone; Z-VAD-FMK, benzyloxycarbonyl-Val-Ala-Asp-fluoromethylketone; Z-LEHD-FMK, benzyloxycarbonyl-Leu-Glu-His-Asp-fluoromethylketone; TNF-α, tumor necrosis factor-α; LDH, lactate dehydrogenase; NAC, N-acetyl cysteine; BSO, L-buthionine sulfoximine; FITC, fluorescein isothiocyanate; MMP ($\Delta\Psi_m$), mitochondrial membrane potential; MTT, 3-(4,5-dimethylthiazol-2-yl)-2,5-diphenyltetrazolium bromide; PI, propidium iodide; $H_2$DCFDA, 2',7'-dichlorodihydrofluorescein diacetate; CMFDA, 5-chloromethylfluorescein diacetate

*Key words:* valproic acid, histone deacetylase, apoptosis, HeLa, caspase

## Introduction

Histone deacetylase (HDAC) is a class of enzymes that removes acetyl groups from lysine amino acid on histone, leading to the control of transcription (1). Dysregulation of HDAC activity causes the silence of tumor suppressor genes such as p53 and contributes to cancer initiation and development (2,3). It was reported that HDAC activity and expression are increased in several types of human cancer, including breast and prostate cancer (4,5). Therefore, HDAC inhibitors can be considered as novel strategic agents in cancer therapeutics. In fact, vorinostat and romidepsin have been used for the treatment of cutaneous T-cell lymphoma (6). HDAC inhibitors have been known to induce cell cycle arrest, cell differentiation, apoptotic and autophagic cell death in various cancer cells (7-9). In addition, it is reported that HDAC inhibitor and tumor necrosis factor (TNF)-family members synergistically induce apoptosis in many cancer cells such as breast, liver and lymphoma cells (10-12). HDAC inhibitors also generate reactive oxygen species (ROS) in solid tumor and leukemia cells (13). Excessive production of ROS, known as oxidative stress, has been recognized to induce cell death.

Cervical cancer is a major cause of mortality in women worldwide and its occurrence results from both genetic and epigenetic events. Overexpression of HDAC2 is observed in cervical cancer cells (14). Furthermore, it was reported that the acetylated form of histone H3 in cytologic smears is related to the progression of cervical cancer (15). Originally, valproic acid (VPA) was clinically used in epilepsy and bipolar disorder. However, it was recently reported that VPA has an anticancer effect on ovarian and liver cancer cells *in vitro* and *in vivo* (16,17). However, little is known about the anticancer effect of VPA on cervical cancer cells in view of changes in ROS and GSH levels. Therefore, in the present study, we investigated the effects of VPA on cell growth and death in human cervical HeLa cells in relation to ROS and GSH levels.

## Materials and methods

*Cell culture.* Human cervix adenocarcinoma HeLa cells were obtained from the American Type Culture Collection (ATCC; Manassas, VA, USA) and maintained in a humidified incubator containing 5% $CO_2$ at 37˚C. The HeLa cells were cultured in RPMI-1640 medium (Sigma-Aldrich, St. Louis, MO, USA)

supplemented with 10% fetal bovine serum (FBS; Sigma-Aldrich) and 1% penicillin-streptomycin (Gibco-BRL, Grand Island, NY, USA). The cells were routinely grown in 100-mm plastic tissue culture dishes (Nunc, Roskilde, Denmark) and harvested with a solution of trypsin-EDTA while in a logarithmic phase of growth.

*Reagents*. The VPA was purchased from Sigma-Aldrich, and was dissolved in water at 1 M as a stock solution. The pan-caspase inhibitor (Z-VAD-FMK; benzyloxycarbonyl-Val-Ala-Asp-fluoromethylketone), the caspase-3 inhibitor (Z-DEVD-FMK; benzyloxycarbonyl-Asp-Glu-Val-Asp-fluoromethylketone), the caspase-8 inhibitor (Z-IETD-FMK; benzyloxycarbonyl-Ile-Glu-Thr-Asp-fluoromethylketone) and the caspase-9 inhibitor (Z-LEHD-FMK; benzyloxycarbonyl-Leu-Glu-His-Asp-fluoromethylketone) were obtained from R&D Systems, Inc. (Minneapolis, MN, USA) and were dissolved in DMSO at 10 mM to serve as stock solutions. TNF-α was also obtained from R&D Systems and were dissolved in water at 10 μg/ml as a stock solution. NAC and BSO were also obtained from Sigma-Aldrich, and NAC was dissolved in buffer [20 mM HEPES (pH 7.0)] at 100 mM as a stock solution. BSO was dissolved in water at 100 mM as a stock solution. Cells were pretreated with 15 μM caspase inhibitors, 2 mM NAC or 100 μM BSO for 1 h prior to VPA treatment.

*Growth inhibition assay*. The effect of VPA on cell growth was determined by measuring 3-(4,5-dimethylthiazol-2-yl)-2,5-diphenyltetrazolium bromide (MTT; Sigma-Aldrich) absorbance in living cells, as previously described (18). In brief, $5x10^3$ cells were seeded in 96-well microtiter plates (Nunc) for MTT assays. After exposure to the designated doses of VPA for the indicated times, MTT solution [20 ml: 2 mg/ml in phosphate-buffered saline (PBS)] was added to each well of the 96-well plates. The plates were additionally incubated for 3 h at 37˚C. Medium was withdrawn from the plates by pipetting and 200 ml DMSO was added to each well to solubilize the formazan crystals. The optical density was measured at 570 nm using a microplate reader (Synergy™ 2, BioTek Instruments Inc., Winooski, VT, USA).

*Nuclear/cytosol fractionation*. The isolation of nuclear and cytosol extract was performed with the nuclear/cytosol fractionation kit (BioVision, San Francisco, CA, USA) according to the manufacturer's instructions. In brief, $1x10^6$ cells in a 60-mm culture dish (Nunc) were incubated with the indicated doses of VPA for 24 h. The cells were then washed in PBS and suspended in 200 μl cytosol extraction buffer provided with the kit on ice for 10 min. After 5 min centrifugation, the supernatant (cytosol fraction) was collected and the pellets were resuspended in the nuclear extraction buffer provided with the kit. Protein concentrations were determined using the Bradford method.

*Measurement of HDAC activity*. HDAC activity was assessed using the HDAC assay kit (Millipore, Billerica, MA, USA) according to the manufacturer's instructions. In brief, $1x10^6$ cells in a 60-mm culture dish (Nunc) were incubated with the indicated doses of VPA for 24 h. The cells were then washed in PBS and suspended in 5 volumes of lysis buffer (R&D Systems). Protein concentrations were determined using the Bradford method. Supernatant samples containing 30 μg of total, cytosol and nuclear protein were used for determination of HDAC activity. These samples were added to each well in 96-well microtiter plates (Nunc) with HDAC substrate provided by the assay kit at 37˚C for 1 h. The optical density of each well was measured at 405 nm using a microplate reader (Synergy™ 2; BioTek Instruments).

*Western blot analysis*. The expression of proteins was evaluated using western blot analysis, as previously described (19). In brief, $1x10^6$ cells in a 60-mm culture dish (Nunc) were incubated with the designated doses of VPA for 24 h. The cells were then washed in PBS and suspended in five volumes of lysis buffer (20 mM HEPES, pH 7.9, 20% glycerol, 200 mM KCl, 0.5 mM EDTA, 0.5% NP40, 0.5 mM DTT, 1% protease inhibitor cocktail). Supernatant protein concentrations were determined using the Bradford method. Supernatant samples containing 30 μg total protein were resolved by 15% SDS-PAGE gels depending on the sizes of target proteins, transferred to Immobilon-P PVDF membranes (Millipore) by electroblotting, and then probed with anti-acetylated H3 (Millipore), anti-PARP, anti-c-PARP, anti-Bcl-2 (Cell Signaling Technology Inc., Danvers, MA, USA) anti-β-actin antibodies (Santa Cruz Biotechnology, Santa Cruz, CA, USA). Membranes were incubated with horseradish peroxidase-conjugated secondary antibodies. Blots were developed using an ECL kit (Amersham, Arlington Heights, IL, USA).

*Cell cycle and sub-G1 cell analysis*. Cell cycle and sub-G1 cell analysis were determined by propidium iodide (PI, Ex/Em = 488/617 nm; Sigma-Aldrich) staining, as previously described (20). In brief, $1x10^6$ cells in a 60-mm culture dish (Nunc) were incubated with the designated doses of VPA with or without 15 μM caspase inhibitors, 2 mM NAC or 100 μM BSO for 24 h. Cells were washed again with PBS, then incubated with PI (10 μg/ml) with simultaneous RNase treatment at 37˚C for 30 min. Cellular DNA content was measured using a FACStar flow cytometer (Becton-Dickinson, Franklin Lakes, NJ, USA) and analyzed by using Lysis II and CellFit software (Becton-Dickinson).

*Annexin V-FITC/PI staining for cell death detection*. Apoptotic cell death was determined by staining cells with Annexin V-fluorescein isothiocyanate (FITC; Invitrogen Life Technologies, Camarillo, CA, USA; Ex/Em = 488/519 nm), as previously described (20). In brief, $1x10^6$ cells in a 60-mm culture dish (Nunc) were incubated with the designated doses of VPA with or without 15 μM caspase inhibitors, 10 ng/ml TNF-α, 2 mM NAC or 100 μM BSO for 24 h. Cells were washed twice with cold PBS and then resuspended in 500 μl of binding buffer (10 mM HEPES/NaOH pH 7.4, 140 mM NaCl, 2.5 mM $CaCl_2$) at a concentration of $1x10^6$ cells/ml. Annexin V-FITC (5 μl) and PI (1 μg/ml) were then added and the cells were analyzed with a FACStar flow cytometer.

*Quantification of caspase-3, -8 and -9 activity*. The activity of caspase-3, -8 and -9 was assessed using the caspase-3, -8 and -9 colorimetric assay kits (R&D Systems), respectively (21). In brief, $1x10^6$ cells in a 60-mm culture dish (Nunc) were incu-

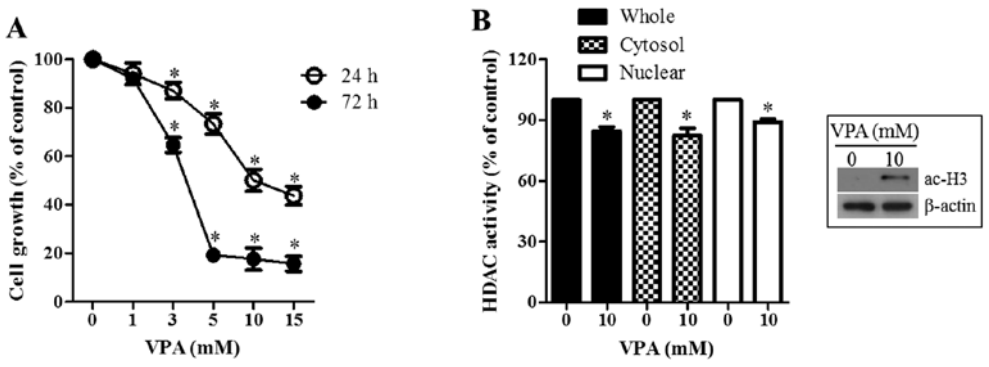


Figure 1. Effects of VPA on cell growth and HDAC activity in HeLa cells. Exponentially growing cells were treated with the designated concentrations of VPA for the indicated times. (A) The graph shows cellular growth changes in HeLa cells, as assessed by MTT assay. (B) The graph shows HDAC activity in HeLa cells. The inset indicates the level of acetylated H3 protein in VPA-treated HeLa cells. *P<0.05 compared with the control group.

bated with 10 mM VPA for 24 h. The cells were then washed in PBS and suspended in 5 volumes of lysis buffer provided with the kit. Protein concentrations were determined using the Bradford method. Supernatants containing 50 $\mu$g total protein were used to determine caspase-3, -8 and -9 activities. The supernatants were added to each well in 96-well microtiter plates (Nunc) with DEVD-pNA, IETD-pNA or LEHD-pNA as caspase-3, -8 and -9 substrates and the plates were incubated at 37˚C for 1 h. The optical density of each well was measured at 405 nm using a microplate reader (Synergy™ 2; BioTek Instruments). The activity of caspase-3, -8 and -9 was expressed in arbitrary absorbance units.

*Measurement of MMP ($\Delta\Psi_m$).* The MMP ($\Delta\Psi_m$) levels were measured by a Rhodamine 123 fluorescent dye (Sigma-Aldrich; Ex/Em = 485/535 nm) as previously described (20,22). In brief, $1x10^6$ cells in a 60-mm culture dish (Nunc) were incubated with the designated doses of VPA for 24 h. Cells were washed twice with PBS and incubated with Rhodamine 123 (0.1 $\mu$g/ml) at 37˚C for 30 min. Rhodamine 123 staining intensity was determined by a FACStar flow cytometer. The cells that were Rhodamine 123 negative were indicated to have lost MMP ($\Delta\Psi_m$). MMP ($\Delta\Psi_m$) levels in cells except MMP ($\Delta\Psi_m$) loss cells were expressed as mean fluorescence intensity (MFI), which was calculated by the CellQuest software.

*Lactate dehydrogenase (LDH) activity for the detection of necrosis.* Necrosis in cells treated with VPA and/or TNF-α was evaluated by an LDH kit (Sigma-Aldrich). In brief, $1x10^6$ cells in a 60-mm culture dish (Nunc) were incubated with the indicated doses of VPA and/or TNF-α for 24 h. After treatment, the culture media were collected and centrifuged for 5 min at 1,500 rpm. Media supernatant (50 $\mu$l) was added to a fresh 96-well plate along with LDH assay reagent and then incubated at room temperature for 30 min. The absorbance values were measured at 490 nm using a microplate reader. LDH release was expressed as the percentage of extracellular LDH activity compared with the control cells.

*Detection of intracellular ROS level.* Intracellular ROS such as $H_2O_2$, $^{\bullet}OH$ and $ONOO^{\bullet}$ was detected by means of an oxidation-sensitive fluorescent probe dye, 2',7'-dichlorodihydrofluorescein diacetate ($H_2$DCFDA, Invitrogen Molecular Probes, Eugene, OR, USA; Ex/Em = 495 nm/529 nm) (20). In brief, $1x10^6$ cells in a 60-mm culture dish (Nunc) were incubated with the designated doses of VPA for the indicated times. Cells were then washed in PBS and incubated with 20 $\mu$M $H_2$DCFDA at 37˚C for 30 min. DCF fluorescence was detected using a FACStar flow cytometer. ROS level was expressed as MFI, which was calculated by the CellQuest software (Becton-Dickinson).

*Detection of intracellular GSH level.* Cellular GSH levels were analyzed using a 5-chloromethylfluorescein diacetate dye (CMFDA, Ex/Em = 522/595 nm; Invitrogen Life Technologies) as previously described (23). In brief, $1x10^6$ cells were incubated in a 60-mm culture dish (Nunc) with the designated doses of VPA with or without 2 mM NAC or 100 $\mu$M BSO for 24 h. Cells were then washed with PBS and incubated with 5 $\mu$M CMFDA at 37˚C for 30 min. CMF fluorescence intensity was determined using a FACStar flow cytometer. Negative CMF staining (GSH depletion) of cells was expressed as the percentage of (-) CMF cells.

*Statistical analysis.* The results represent the mean of at least three independent experiments (mean ± SD). Data were analyzed using InStat software (GraphPad Prism 4; GraphPad San Diego, CA, USA). The Student's t-test or one-way analysis of variance (ANOVA) with post hoc analysis using Tukey's multiple comparison test was used for parametric data. P<0.05 was considered to indicate a statistically significant difference.

## Results

*Effects of VPA on cell growth and HDAC activity in HeLa cells.* The effect of VPA on the growth inhibition of HeLa cells was examined using MTT assays. After exposure to the various concentrations of VPA for various times, HeLa cell growth was dose- and time-dependently decreased with an $IC_{50}$ of ~10 and 4 mM at 24 and 72 h, respectively (Fig. 1A). When testing whether VPA as a HDAC inhibitor indeed inhibited HDAC activity, VPA significantly attenuated the activities of total, cytosol and nuclear HDACs at 24 h (Fig. 1B). Furthermore, it was observed that VPA increased the form of acetylated histone 3 in HeLa cells (Fig. 1B).

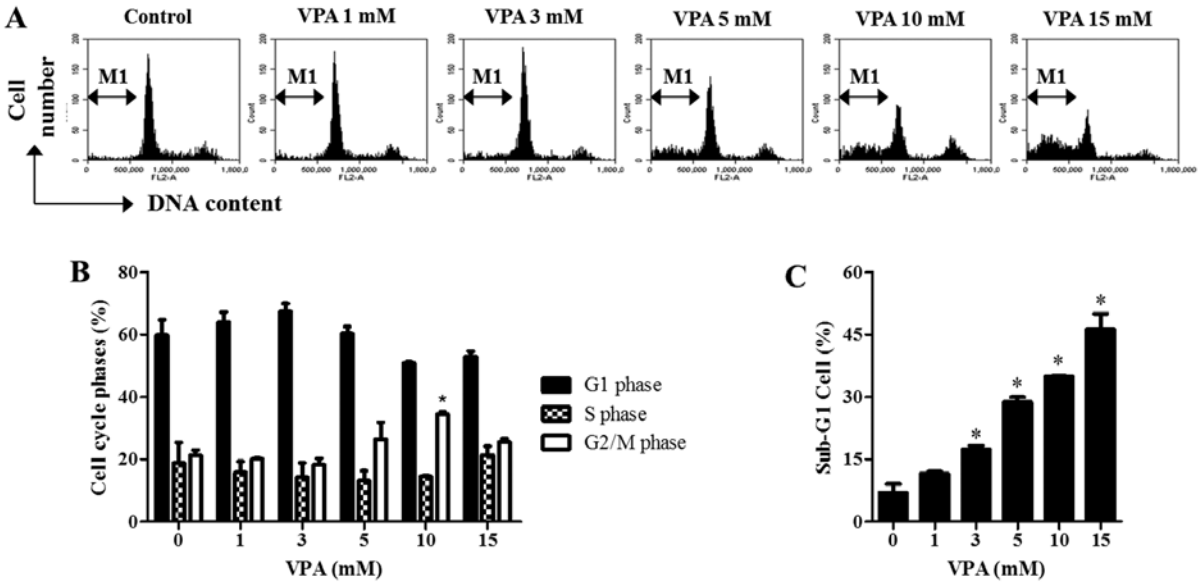


Figure 2. Effects of VPA on cell cycle distribution and sub-G1 cells in HeLa cells. Exponentially growing cells were treated with the indicated concentrations of VPA for 24 h. (A) The changes of cell cycle phase distribution and sub-G1 cells were assessed by DNA flow cytometric analysis. (B) The graph indicates changes in the cell cycle distribution as assessed by DNA flow cytometric analysis. (C) The graph shows the percentage of sub-G1 cells. *P<0.05 compared with the control group.

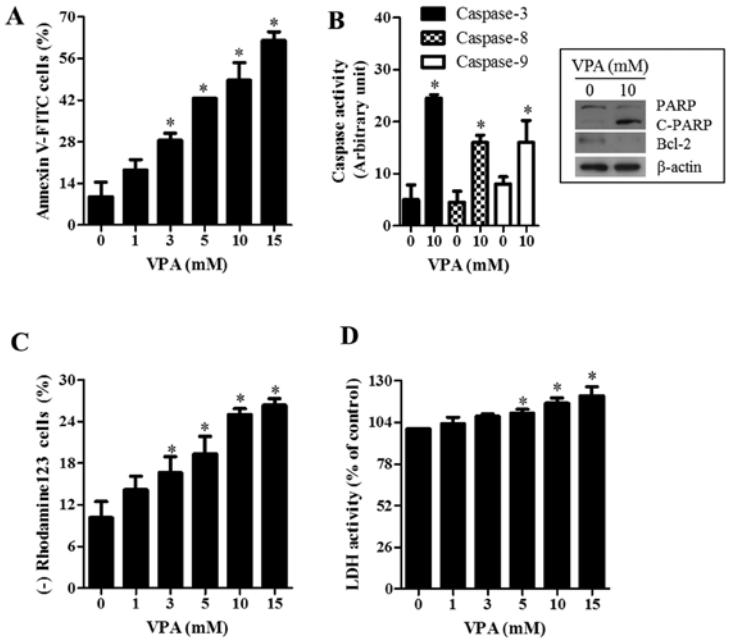


Figure 3. Effects of VPA on cell death, MMP ($\Delta\Psi_m$) and LDH release in HeLa cells. Exponentially growing cells were treated with the indicated concentrations of VPA for 24 h. (A) The graph shows the percentage of Annexin V positive cells as measured by FACStar flow cytometer. (B) The graph shows the activity of caspase-3, -8 and -9 in VPA-treated cells. The inset indicates the levels of PARP, c-PARP and Bcl-2 proteins in VPA-treated HeLa cells. (C) The graph indicates the percentage of Rhodamine 123-negative [MMP ($\Delta\Psi_m$) loss] cells. (D) The graph shows the percentage of LDH release compared with that in the control cells. *P<0.05 compared with the control group.

*Effects of VPA on cell cycle distribution and sub-G1 cells in HeLa cells*. Since the growth inhibition of HeLa cells by VPA could be explained by an arrest during the cell cycle progression, cell cycle distributions were examined at 24 h. As shown in Fig. 2A and B, DNA flow cytometric analysis indicated that 1-3 mM VPA seemed to induce a G1 phase arrest while 10 mM VPA significantly induced a G2/M phase arrest of cell cycle in HeLa cells. In addition, VPA increased the percentage of sub-G1 cells in HeLa cells in a dose-dependent manner at 24 h (Fig. 2A and C).

*Effects of VPA on cell death, MMP ($\Delta\Psi_m$) and LDH release in HeLa cells*. VPA also increased the number of Annexin V-FITC positive cells in HeLa cells (Fig. 3A). In

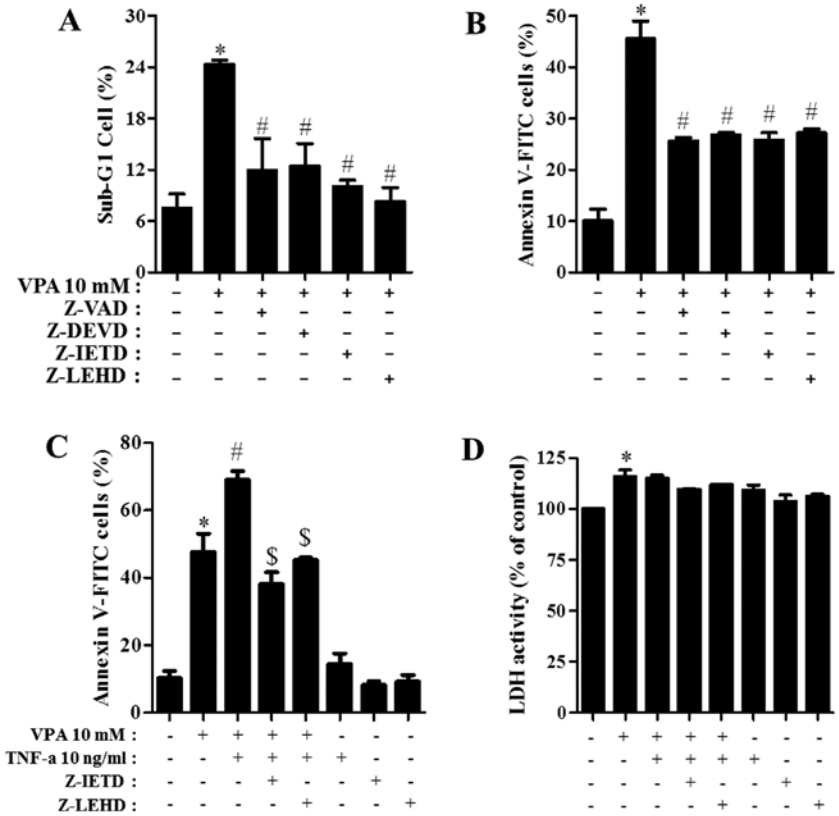


Figure 4. Effects of caspase inhibitors and TNF-α in VPA-treated HeLa cells. Exponentially growing cells were treated with 10 mM VPA, 15 $\mu$M caspase inhibitors and/or 10 ng/ml TNF-α for 24 h. (A and B) The graphs show the percentage of sub-G1 cells and Annexin V-positive cells, respectively. (C and D) The graphs indicate the percentage of Annexin V-positive cells and LDH release compared with that in the control cells, respectively. $^{*}$P<0.05 compared with the control group. $^{\#}$P<0.05 compared with cells treated with VPA only. $^{\$}$P<0.05 compared with cells co-treated with VPA and TNF-α.

addition, the activity of caspase-3, -8 and -9 was increased in 10 mM VPA-treated HeLa cells (Fig. 3B). The examination of the expressions in apoptotic-related proteins showed that the intact form of poly (ADP-ribose) polymerase (PARP) was reduced and instead its cleavage form was induced by VPA (Fig. 3B). The level of Bcl-2 was also downregulated by VPA in HeLa cells (Fig. 3B). Cell death is closely related to the collapse of the MMP ($\Delta\Psi_m$) (24). As expected, loss of MMP ($\Delta\Psi_m$) was observed in VPA-treated HeLa cells (Fig. 3C). Since VPA induced necrosis in HeLa cells, the status of necrosis was assessed using an LDH release. Treatment with 5-15 mM VPA significantly increased LDH release (Fig. 3D).

*Effects of caspase inhibitors and TNF-α in VPA-treated HeLa cells*. It was determined which caspases were involved in the death of VPA-treated HeLa cells. For this experiment, we chose 10 mM VPA as a suitable dose to differentiate the level of cell death in the presence or absence of each caspase inhibitor [pan-caspase inhibitor (Z-VAD), caspase-3 inhibitor (Z-DEVD), caspase-8 inhibitor (Z-IETD), or caspase-9 inhibitor (Z-LEHD)]. A concentration of 15 $\mu$M of each caspase inhibitor was used as an optimal dose since it did not affect cell death in the control HeLa cells (25). All the caspase inhibitors attenuated the percentage of sub-G1 cells in VPA-treated HeLa cells (Fig. 4A) and they prevented apoptotic cell death in these cells (Fig. 4B). Therefore, the activation of various caspases seemed to be involved in apoptotic HeLa cell death caused by VPA. Moreover, TNF-α enhanced apoptotic cell death in VPA-treated HeLa cells (Fig. 4C). When Z-IETD (caspase-8 inhibitor) or Z-LEHD (caspase-9 inhibitor) was co-incubated in HeLa cells co-treated with VPA and TNF-α, these inhibitors significantly prevented apoptosis caused by co-treatment with VPA and TNF-α (Fig. 4C). However, TNF-α did not augment LDH release in VPA-treated and -untreated HeLa cells (Fig. 4D). Neither Z-IETD nor Z-LEHD affected LDH release in VPA-treated and -untreated HeLa cells (Fig. 4D).

*Effects of NAC and BSO on cell death, ROS and GSH levels in VPA-treated HeLa cells*. Changes in the intracellular ROS and GSH levels were investigated in HeLa cells treated with VPA. VPA significantly increased the intracellular ROS (DCF) level in HeLa cells from 30 min to 24 h. In relation to GSH level, VPA significantly increased GSH-depleted cell number at 24 h in a dose-dependent manner (Fig. 5B). Next, the effects of NAC (an antioxidant) or BSO (an inhibitor of GSH synthesis) on cell death were examined in VPA-treated HeLa cells. As shown in Fig. 5C and D, NAC and BSO did not affect cell death induced by VPA. When assessing whether NAC or BSO influences ROS level in VPA-treated HeLa cells, NAC slightly reduced ROS levels in these cells and BSO significantly increased ROS levels in VPA-treated and -untreated HeLa cells (Fig. 5E). Regarding GSH levels, NAC slightly attenuated GSH depletion induced by VPA in HeLa cells (Fig. 5F). BSO seemed to increase GSH depletion in VPA-treated HeLa cells (Fig. 5F).

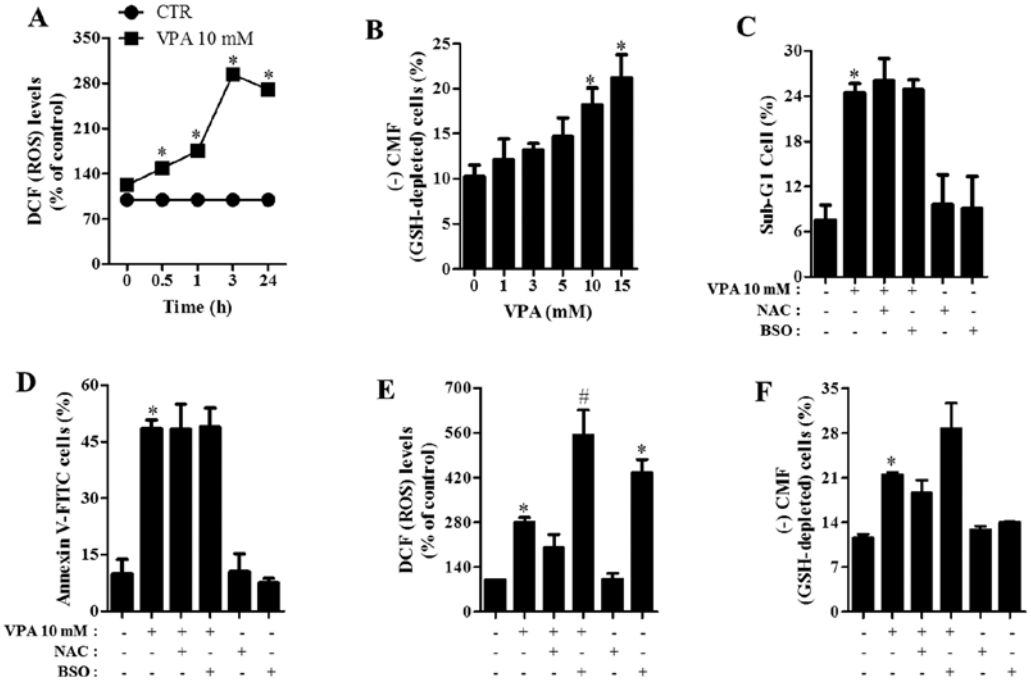


Figure 5. Effects of NAC and BSO on cell death, ROS and GSH levels in VPA-treated HeLa cells. Exponentially growing cells were treated with the indicated concentrations of VPA, 2 mM NAC and/or 100 $\mu$M BSO for the indicated times. ROS and GSH levels in cells were measured with FACStar flow cytometer. (A) The graph shows DCF (ROS) levels compared with those in the control cells. (B) The graph shows the percentage of (-) CMF (GSH-depleted) cells. (C and D) The graphs show the percentage of sub-G1 cells (C) and Annexin V-positive cells (D). (E and F) The graphs indicate DCF (ROS) levels (E) and the percentage of (-) CMF (GSH-depleted) cells (F). $^{*}$P<0.05 compared with the control group. $^{\#}$P<0.05 compared with cells treated with VPA only.

## Discussion

In the present study, we assessed the effects of VPA on HeLa cervical cancer cells in relation to cell death, ROS and GSH levels. VPA inhibited the activities of cytosol and nuclear HDACs in HeLa cells. These results support that VPA is a class 1 and 2 HDAC inhibitor (26). VPA decreased the growth of HeLa cells in dose- and time-dependent manners. When the cell cycle distributions were examined, 10 mM VPA induced a G2/M phase arrest of the cell cycle in HeLa cells at 24 h. However, relatively lower concentrations of VPA seemed to induce a G1 phase arrest in HeLa cells. Similarly, VPA induced a G1 phase or a G2/M phase arrest in gastric cancer and glioblastoma cells (27,28). Therefore, cell cycle arrest in VPA-treated cells was an underlying mechanism to suppress the growth of cancer cells including HeLa cells.

VPA also increased the number of sub-G1 cells and induced apoptosis, which was accompanied by the cleavage of PARP, caspase-3, -8 and -9 activations. Apoptosis is closely related to the collapse of MMP ($\Delta\Psi_m$) (29). Our results demonstrated that VPA triggered the loss of MMP ($\Delta\Psi_m$) in HeLa cells in a dose-dependent manner. Moreover, caspase inhibitors significantly prevented HeLa cell death caused by VPA. These data suggest that the mitochondrial pathway as well as the cell death receptor pathway are all together necessary for the induction of apoptosis in VPA-treated HeLa cells. It is reported that HDAC inhibitor and TNF-family members, especially TRAIL, synergistically induce apoptosis in several cancer cells such as breast, liver and lymphoma cells (10-12). According to the present study, TNF-α synergistically enhanced cell death in VPA-treated HeLa cells. Treatment with TRAIL or FasL did not affect cell death induced by VPA in HeLa cells (data not shown). Although VPA induced LDH release, TNF-α did not enhance this release in VPA-treated HeLa cells. This result indicates that HeLa cell death caused by VPA and/or TNF-α did not result from the necrotic pathway. In particular, Z-IETD and Z-LEHD significantly attenuated HeLa cell death induced by co-treatment with VPA and TNF-α. Furthermore, we observed that VPA induced autophagy, as evidenced by the conversion of LC3-I to LC3-II (data not shown). However, autophagy inhibitors, hydroxychloroquinine and 3-methyladenine did not affect HeLa cell death induced by VPA. Taken together, the main cause of HeLa cell death induced by VPA is mediated by apoptosis rather than necrotic or autophagic cell death.

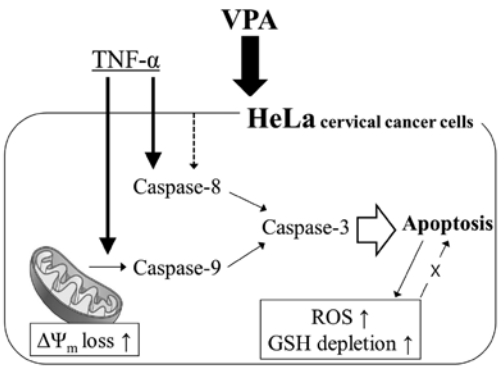


Figure 6. Schematic diagram of VPA-induced HeLa cell death.

HDAC inhibitors generate ROS in solid tumor and leukemia cells and induce apoptosis in these cells (30). Oxidative stress might be involved in HDAC inhibitor-induced cell death. It is reported that NAC prevents cell death induced by HDAC

inhibitors (31). Similarly, ROS levels significantly increased in VPA-treated HeLa cells from 30 min to 24 h. However, NAC did not attenuate cell death level in VPA-treated HeLa cells at 24 h. Since NAC decreased ROS levels in VPA-treated HeLa cells, this agent seemed to work as an antioxidant in these cells. In addition, although BSO increased ROS levels in VPA-treated and -untreated HeLa cells, it did not enhance cell death. Therefore, VPA-induced HeLa cell death was not closely related to ROS. The increased ROS level induced by VPA seems to be a byproduct of VPA-induced HeLa cell death.

GSH is an important intracellular antioxidant that protects cells from damage caused by free radical and toxins. It is able to clear away $O2^{\bullet-}$ and provide electrons for glutathione peroxidase to reduce $H_2O_2$ to $H_2O$. Apoptotic effects are inversely comparative to GSH content (32-34). Similarly, VPA increased the percentage of GSH-depleted cells in HeLa cells. NAC slightly decreased GSH depletion whereas BSO augmented it in VPA-treated HeLa cells. However, these agents did not affect cell death induced by VPA in HeLa cells. Therefore, the loss of GSH content seemed to be necessary but not sufficient to fully induce apoptosis in VPA-treated HeLa cells.

In summary, as depicted in Fig. 6, VPA inhibited the growth of HeLa cervical cancer cells via caspase-dependent apoptosis. TNF-α enhanced HeLa apoptotic cell death induced by VPA. The growth inhibition was not dependent on ROS and GSH level changes.

## Acknowledgements

The present study was supported by the National Research Foundation of Korea (NRF) grant funded by the Korean government through the Diabetes Research Center at Chonbuk National University (2012-0009323) and the Basic Science Research Program through the National Research Foundation of Korea (NRF) funded by the Ministry of Education (2013006279).

## References

1. Icardi L, De Bosscher K and Tavernier J: The HAT/HDAC interplay: multilevel control of STAT signaling. Cytokine Growth Factor Rev 23: 283-291, 2012.
2. Lu Z, Luo RZ, Peng H, *et al*: E2F-HDAC complexes negatively regulate the tumor suppressor gene ARHI in breast cancer. Oncogene 25: 230-239, 2006.
3. Khan O and La Thangue NB: HDAC inhibitors in cancer biology: emerging mechanisms and clinical applications. Immunol Cell Biol 90: 85-94, 2012.
4. Cebrian A, Pharaoah PD, Ahmed S, *et al*: Genetic variants in epigenetic genes and breast cancer risk. Carcinogenesis 27: 1661-1669, 2006.
5. Wang L, Zou X, Berger AD, *et al*: Increased expression of histone deacetylaces (HDACs) and inhibition of prostate cancer growth and invasion by HDAC inhibitor SAHA. Am J Transl Res 1: 62-71, 2009.
6. Robey RW, Chakraborty AR, Basseville A, *et al*: Histone deacetylase inhibitors: emerging mechanisms of resistance. Mol Pharm 8: 2021-2031, 2011.
7. Pettazzoni P, Pizzimenti S, Toaldo C, *et al*: Induction of cell cycle arrest and DNA damage by the HDAC inhibitor panobinostat (LBH589) and the lipid peroxidation end product 4-hydroxynonenal in prostate cancer cells. Free Radic Biol Med 50: 313-322, 2011.
8. Frumm SM, Fan ZP, Ross KN, *et al*: Selective HDAC1/HDAC2 inhibitors induce neuroblastoma differentiation. Chem Biol 20: 713-725, 2013.
9. Rikiishi H: Autophagic and apoptotic effects of HDAC inhibitors on cancer cells. J Biomed Biotechnol 2011: 830260, 2011.
10. Lauricella M, Ciraolo A, Carlisi D, *et al*: SAHA/TRAIL combination induces detachment and anoikis of MDA-MB231 and MCF-7 breast cancer cells. Biochimie 94: 287-299, 2012.
11. Carlisi D, Lauricella M, D'Anneo A, *et al*: The histone deacetylase inhibitor suberoylanilide hydroxamic acid sensitises human hepatocellular carcinoma cells to TRAIL-induced apoptosis by TRAIL-DISC activation. Eur J Cancer 45: 2425-2438, 2009.
12. Al-Yacoub N, Fecker LF, Mobs M, *et al*: Apoptosis induction by SAHA in cutaneous T-cell lymphoma cells is related to downregulation of c-FLIP and enhanced TRAIL signaling. J Invest Dermatol 132: 2263-2274, 2012.
13. Gong K, Xie J, Yi H and Li W: CS055 (Chidamide/HBI-8000), a novel histone deacetylase inhibitor, induces G1 arrest, ROS-dependent apoptosis and differentiation in human leukaemia cells. Biochem J 443: 735-746, 2012.
14. Huang BH, Laban M, Leung CH, *et al*: Inhibition of histone deacetylase 2 increases apoptosis and $p21^{Cip1/WAF1}$ expression, independent of histone deacetylase 1. Cell Death Differ 12: 395-404, 2005.
15. Anton M, Horky M, Kuchtickova S, *et al*: Immunohistochemical detection of acetylation and phosphorylation of histone H3 in cervical smears. Ceska Gynekol 69: 3-6, 2004.
16. Shan Z, Feng-Nian R, Jie G and Ting Z: Effects of valproic acid on proliferation, apoptosis, angiogenesis and metastasis of ovarian cancer in vitro and in vivo. Asian Pac J Cancer Prev 13: 3977-3982, 2012.
17. Machado MC, Bellodi-Privato M, Kubrusly MS, *et al*: Valproic acid inhibits human hepatocellular cancer cells growth in vitro and in vivo. J Exp Ther Oncol 9: 85-92, 2011.
18. Han YH, Moon HJ, You BR, *et al*: Effects of carbonyl cyanide p-(trifluoromethoxy) phenylhydrazone on the growth inhibition in human pulmonary adenocarcinoma Calu-6 cells. Toxicology 265: 101-107, 2009.
19. You BR and Park WH: Zebularine inhibits the growth of HeLa cervical cancer cells via cell cycle arrest and caspase-dependent apoptosis. Mol Biol Rep 39: 9723-9731, 2012.
20. Han YH, Moon HJ, You BR and Park WH: The effect of MG132, a proteasome inhibitor on HeLa cells in relation to cell growth, reactive oxygen species and GSH. Oncol Rep 22: 215-221, 2009.
21. You BR and Park WH: Proteasome inhibition by MG132 induces growth inhibition and death of human pulmonary fibroblast cells in a caspase-independent manner. Oncol Rep 25: 1705-1712, 2011.
22. Han YH, Kim SH, Kim SZ and Park WH: Carbonyl cyanide p-(trifluoromethoxy) phenylhydrazone (FCCP) as an O2(*-) generator induces apoptosis via the depletion of intracellular GSH contents in Calu-6 cells. Lung Cancer 63: 201-209, 2009.
23. Han YH and Park WH: Propyl gallate inhibits the growth of HeLa cells via regulating intracellular GSH level. Food Chem Toxicol 47: 2531-2538, 2009.
24. Griffiths EJ: Mitochondria - potential role in cell life and death. Cardiovasc Res 46: 24-27, 2000.
25. You BR and Park WH: Suberoyl bishydroxamic acid-induced apoptosis in HeLa cells via ROS-independent, GSH-dependent manner. Mol Biol Rep 40: 3807-3816, 2013.
26. Gurvich N, Tsygankova OM, Meinkoth JL and Klein PS: Histone deacetylase is a target of valproic acid-mediated cellular differentiation. Cancer Res 64: 1079-1086, 2004.
27. Zhao X, Yang W, Shi C, *et al*: The G1 phase arrest and apoptosis by intrinsic pathway induced by valproic acid inhibit proliferation of BGC-823 gastric carcinoma cells. Tumour Biol 32: 335-346, 2011.
28. Das CM, Aguilera D, Vasquez H, *et al*: Valproic acid induces p21 and topoisomerase-II (α/β) expression and synergistically enhances etoposide cytotoxicity in human glioblastoma cell lines. J Neurooncol 85: 159-170, 2007.
29. Yang J, Liu X, Bhalla K, *et al*: Prevention of apoptosis by Bcl-2: release of cytochrome c from mitochondria blocked. Science 275: 1129-1132, 1997.
30. Eot-Houllier G, Fulcrand G, Magnaghi-Jaulin L and Jaulin C: Histone deacetylase inhibitors and genomic instability. Cancer Lett 274: 169-176, 2009.
31. Ungerstedt JS, Sowa Y, Xu WS, *et al*: Role of thioredoxin in the response of normal and transformed cells to histone deacetylase inhibitors. Proc Natl Acad Sci USA 102: 673-678, 2005.
32. Han YH, Kim SZ, Kim SH and Park WH: Enhancement of arsenic trioxide-induced apoptosis in HeLa cells by diethyldithiocarbamate or buthionine sulfoximine. Int J Oncol 33: 205-213, 2008.
33. Estrela JM, Ortega A and Obrador E: Glutathione in cancer biology and therapy. Crit Rev Clin Lab Sci 43: 143-181, 2006.
34. Han YH, Kim SZ, Kim SH and Park WH: Suppression of arsenic trioxide-induced apoptosis in HeLa cells by N-acetylcysteine. Mol Cells 26: 18-25, 2008.